





Cite this: *RSC Adv.*, 2025, 15, 8102

# Discovery of lanthanide metal oxide catalyst for transesterification reaction by fluorescence-based high-throughput screening method and application to biodiesel production†

Jeong Yup Ryoo,  Mingyeong Jang, Taeho Lim  and Min Su Han \*

The development of heterogeneous metal oxide catalysts for transesterification reactions is crucial owing to their seamless reusability and environmental friendliness. In recent years, numerous studies have been conducted on rare-earth oxides, such as lanthanide metal oxides. Various metal oxides were screened for transesterification using a new fluorescence-based high-throughput screening (HTS) method with a pyrene excimer probe, bis(4-(1-pyrenyl)butyl) maleate (BPBM). Praseodymium(IV) oxide (PrO<sub>2</sub>) yielded the highest catalytic activity among the prepared metal oxides. Various substrates were successfully transesterified, and biodiesel was produced in a high yield (90%) from soybean oil through transesterification using the catalyst. The selected catalyst required minimal amounts for the transesterification of various organic substrates (0.7 mol%) and soybean oil (0.8 wt%).

Received 2nd December 2024

Accepted 26th February 2025

DOI: 10.1039/d4ra08489f

rsc.li/rsc-advances

## Introduction

Transesterification is a fundamental organic reaction in which an ester reacts with an alcohol to form a different ester and alcohol. The reaction is used in organic synthesis to obtain various complex ester molecules from commercially available methyl esters and in industrial applications, such as polymers and paints.<sup>1</sup> Various types of catalysts that promote transesterification have been studied, including Lewis acids,<sup>2–6</sup> bases,<sup>7–10</sup> and N-heterocyclic carbenes.<sup>11–15</sup> Among these, the use of heterogeneous catalysts is advantageous owing to seamless reuse and the resulting environmental friendliness.<sup>3,4</sup>

Metal oxides have been extensively studied as heterogeneous catalysts for transesterification, and the functionalization of esters and carbonates has been achieved using transition metal oxides such as Fe<sub>2</sub>O<sub>3</sub>-ZnO,<sup>16</sup> ZnO,<sup>17</sup> Cu/V<sub>2</sub>O<sub>5</sub>,<sup>18</sup> and TiO<sub>2</sub> (ref. 19) as catalysts. These transesterification reactions are widely employed for the functionalization of esters, with a notable example being the conversion of vegetable oils or animal fats into fatty acid methyl esters (FAMES) for biodiesel production. Several transition metal oxides have been reported as effective catalysts for biodiesel production through transesterification reactions.<sup>20–24</sup>

Rare earth oxides have recently been utilized in transesterification reactions in addition to conventional transition metal oxides. For example, cerium oxide, a lanthanide element, has been utilized to catalyze transesterification reactions between various esters and alcohols.<sup>25</sup> Moreover, praseodymium has been mixed with titanium oxide (Ti<sub>0.96</sub>Pr<sub>0.04</sub>O<sub>2</sub>) to enhance the transesterification reaction converting propylene carbonate to dimethyl carbonate and propylene glycol.<sup>26</sup> Rare-earth oxide catalysts have also been utilized in the functionalization of glycerides. For instance, transesterification between rapeseed oil and methanol was tested using various rare earth oxides, and La<sub>2</sub>O<sub>3</sub> was identified as an effective catalyst for producing FAMES.<sup>27</sup> The transesterification of corn oil and waste cooking oil was achieved using a rare earth metal oxides-zirconia (La<sub>0.2</sub>Ce<sub>0.8</sub>O<sub>1.9</sub>-ZrO<sub>2</sub>) catalyst,<sup>28</sup> and the conversion efficiency was enhanced by doping the praseodymium to the CaO nanocatalyst extracted from mussel shell.<sup>29</sup> As can be seen in these recent studies, metal oxide catalysts containing rare-earth metals are promising for transesterification.

To develop a catalyst, selecting one with high activity for a target reaction among various catalysts is crucial, and significant effort and time are required to run many reactions and evaluate each catalyst. Therefore, various high-throughput screening (HTS) methods have been developed to improve the efficiency of catalyst and reaction development. However, HTS using traditional analytical methods, such as gas chromatography (GC),<sup>30–32</sup> liquid chromatography (LC),<sup>33,34</sup> mass spectrometry (MS),<sup>35–37</sup> and nuclear magnetic resonance (NMR)<sup>38,39</sup> is disadvantageous owing to the lengthy processing time per sample or high-cost automated equipment. HTS methods using

Department of Chemistry, Gwangju Institute of Science and Technology (GIST), 123, Cheomdangwagi-ro, Buk-gu, Gwangju, 61005, Republic of Korea. E-mail: happyhan@gist.ac.kr

† Electronic supplementary information (ESI) available: Elemental mapping images of PrO<sub>2</sub> catalyst. Yield calculation of biodiesel production with soybean oil, NMR spectra. See DOI: <https://doi.org/10.1039/d4ra08489f>



colorimetric<sup>40–49</sup> or fluorometric<sup>50–61</sup> responses have been developed, which enable rapid sample processing using relatively inexpensive equipment to overcome these vulnerabilities. Various reactions, such as the Heck reaction,<sup>51</sup> arylation,<sup>52,53</sup> reduction,<sup>58</sup> and coupling reaction<sup>59</sup> have been monitored through fluorescence changes. However, to the best of our knowledge, fluorescence-based monitoring method for transesterification reactions of alkyl esters is not reported.

In this study, various transition or lanthanide metal oxides were prepared to develop rare-earth oxide catalysts for transesterification reactions. The optimal catalyst for transesterification was selected from these catalyst candidates through a newly developed excimer-based fluorescence HTS method. The selected metal oxide catalyst was evaluated for catalytic activity in transesterification across various substrates, including for biodiesel production.

## Experimental section

### Materials and instruments

All chemical reagents were purchased from commercial sources and used as received without further purification. The details about the reagent sources are shown in the ESI.† The instruments used in the experiment included nuclear magnetic resonance (NMR), high-resolution mass spectrometer (HRMS), and fluorescence spectrophotometer. The details about the manufacturer and model of the instrument are shown in the ESI.†

### General procedure for preparation of transition or lanthanide metal oxides

Transition metal or lanthanide metal chlorides (5 mmol) were dissolved in 50 mL of a water/ethanol (3/2, v/v) mixed solvent. An aqueous solution of NaOH (2 g of NaOH in 10 mL of water) was added to the mixture with vigorous stirring. After stirring for 4 h, the suspension mixtures were filtered and washed several times with a water/ethanol (2/1, v/v) mixed solvent until the pH of the filtrate became neutral. Transition or lanthanide metal hydroxide residues were dried in an oven and calcined at 600 °C for 6 h.

**Synthesis of pyrene excimer probe, bis(4-(1-pyrenyl)butyl) maleate (BPBM).** 1-Pyrenebutanol (0.89 g, 3.2 mmol) and maleic anhydride (0.16 g, 1.6 mmol) were dissolved in chloroform (20 mL), and *p*-toluenesulfonic acid (0.06 g, 0.32 mmol) was added. The reaction mixture was heated at reflux overnight, diluted with chloroform, and washed with water. The organic layer was dried over Na<sub>2</sub>SO<sub>4</sub>, and the solvent was removed *in vacuo*. The residue was purified by column chromatography (SiO<sub>2</sub>, CH<sub>2</sub>Cl<sub>2</sub>/hexane = 2/1) to give bis(4-(1-pyrenyl)butyl) maleate (BPBM, 0.89 g, 87%). <sup>1</sup>H NMR (400 MHz, CDCl<sub>3</sub>) δ 8.20–7.78 (m, 18H), 6.22 (s, 2H), 4.17 (t, *J* = 6.5 Hz, 4H), 3.28 (t, *J* = 7.6 Hz, 4H), 1.89–1.72 (m, 8H). HRMS (ESI): *m/z* calculated for C<sub>44</sub>H<sub>37</sub>O<sub>4</sub> [M + H]<sup>+</sup> 629.2686, found 629.2682.

### General procedure for fluorescence-based HTS of transesterification

Bis(4-(1-pyrenyl)butyl) maleate (BPBM, 0.63 mg, 1 μmol) was dissolved in chloroform (0.2 mL), and methanol (0.2 mL,

160 mg, 5 mmol) was added to the solution. Subsequently, transition or lanthanide metal oxide catalysts (10 mg) were added to the solution and refluxed for 24 h. After adding 0.6 mL of chloroform, the reaction mixtures were centrifuged at 600 rpm for 10 min to allow the lanthanide oxide catalyst to settle. The supernatants were diluted 1/10 with chloroform and analyzed using a fluorescence spectrophotometer.

### General procedure for transesterification of aryl esters with alcohols

PrO<sub>2</sub> nanoparticle catalyst (2 mg) was added to the mixtures of esters (1.6 mmol) and alcohols (3.2 mmol), and the reaction mixtures were stirred at 200 °C. The reactions were terminated when the yield exceeded 90% by NMR monitoring aliquots of the twin reaction mixtures of identical compositions for each reaction. The crude products were purified by column chromatography on silica gel to obtain the transesterified ester products.

### Transesterification of glyceryl trioctanoate

A mixture of glyceryl trioctanoate (0.77 g, 1.6 mmol) and methanol (0.52 g, 16 mmol) was placed in a Teflon container, and a PrO<sub>2</sub> nanoparticle catalyst (6 mg) was added to the mixture. The Teflon container containing the reaction mixture was placed in an autoclave and heated at 200 °C for 8 h. The resulting oil was filtered over silica gel and washed with dichloromethane. The solvent and excess methanol were removed *in vacuo* to yield methyl octanoate. <sup>1</sup>H NMR (400 MHz, CDCl<sub>3</sub>) δ 3.66 (s, 3H), 2.30 (t, *J* = 7.6 Hz, 2H), 1.65–1.59 (m, 2H), 1.32–1.26 (m, 8H), 0.88 (t, *J* = 6.8 Hz, 3H).

### Production of biodiesel by transesterification of soybean oil

A mixture of soybean oil (0.8 mL) and methanol (0.52 g, 16 mmol) was placed in a Teflon container, and a PrO<sub>2</sub> nanoparticle catalyst (6 mg) was added to the mixture. The Teflon container containing the reaction mixture was placed in an autoclave and heated at 200 °C for 8 h. The aliquot of the resulting oil was analyzed by <sup>1</sup>H NMR, and the FAME yield was calculated by comparing the peak of the –OCH<sub>3</sub> from FAMES and the peaks of the –OCH<sub>2</sub> from triglycerides.

## Results and discussion

### Development of high-throughput screening method for transesterification with pyrene excimer fluorescent probe

Pyrene is one of the most valuable fluorophores because of its unique excimer behavior, as well as its high quantum yield and lifetime. A probe capable of screening the transesterification reaction was designed based on the significant differences in the fluorescence properties of pyrene excimers and pyrene monomers. However, because pyrene is a fluorophore composed only of aromatic rings with low reactivity, it has the advantage of not causing side reactions other than the target transesterification reaction. Bis(4-(1-pyrenyl)butyl) maleate (BPBM) which bears two pyrenes and linkers to form a pyrene excimer was designed as a fluorescent probe. And this probe can



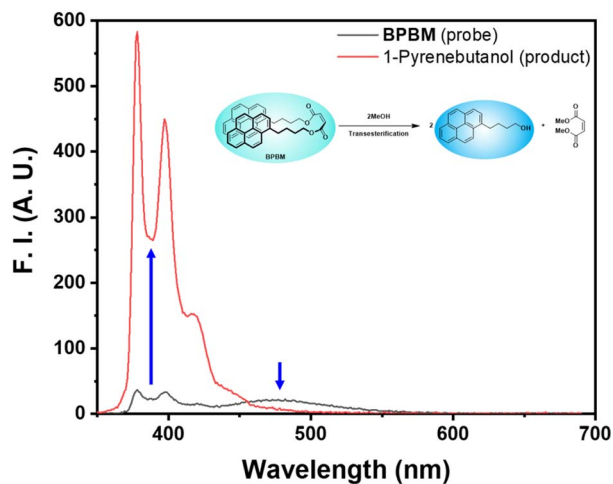


Fig. 1 Comparison of fluorescence spectra between BPBM (pyrene excimer probe) and 1-pyrenebutanol (transesterification product).

be converted into molecules containing only one pyrene by breaking the bond through transesterification at the ester functional groups. Because the pyrene excimer exhibits fluorescence emission at a longer wavelength than the pyrene monomer, a decrease in fluorescence emission at longer wavelengths and an increase at shorter wavelengths are anticipated as the reaction progresses.

The fluorescent probe **BPBM** was synthesized with 87% yield *via* a one-step reaction using 1-pyrenebutanol and maleic anhydride (Fig. S1†). Both **BPBM** and 1-pyrenebutanol were analyzed using a fluorescence spectrophotometer (Fig. 1). 1-Pyrenebutanol, a transesterification product of **BPBM** with alcohols, exhibits a strong fluorescence turn-on characteristic around 390 nm when irradiated with excitation light at 345 nm with respect to **BPBM** before the reaction. Therefore, the progress of the reaction can be effectively determined. Ratiometric analysis was achievable by combining the fluorescence turn-on characteristic at approximately 390 nm and the turn-off characteristic at approximately 480 nm. The fluorescence spectrum exhibits an isoluminescent point at 457 nm, where the fluorescence emission intensity remains constant. This provided self-correction for various analyte-independent factors, such as errors from sample dilution, enabling more precise screening.

The fluorescence spectra of the mixtures containing the **BPBM** probe and 1-pyrenebutanol product were recorded (Fig. 2(a)), yielding a fluorescence calibration curve based on the fluorescence intensity ratios (F. I. at 378 nm F. I. at 480 nm) and mixing ratios (Fig. 2(b)). After transesterification of the **BPBM** probe and methanol using various transition or lanthanide metal oxide catalysts, the reaction mixtures were analyzed using a fluorescence spectrophotometer, and the conversion of the probe and yield of the product was calculated by substituting the fluorescence intensity into the calibration curve.

### High-throughput screening of transition or lanthanide metal oxide catalysts

Eight transition metal oxides and thirteen lanthanide metal oxides were prepared as catalysts following our previous

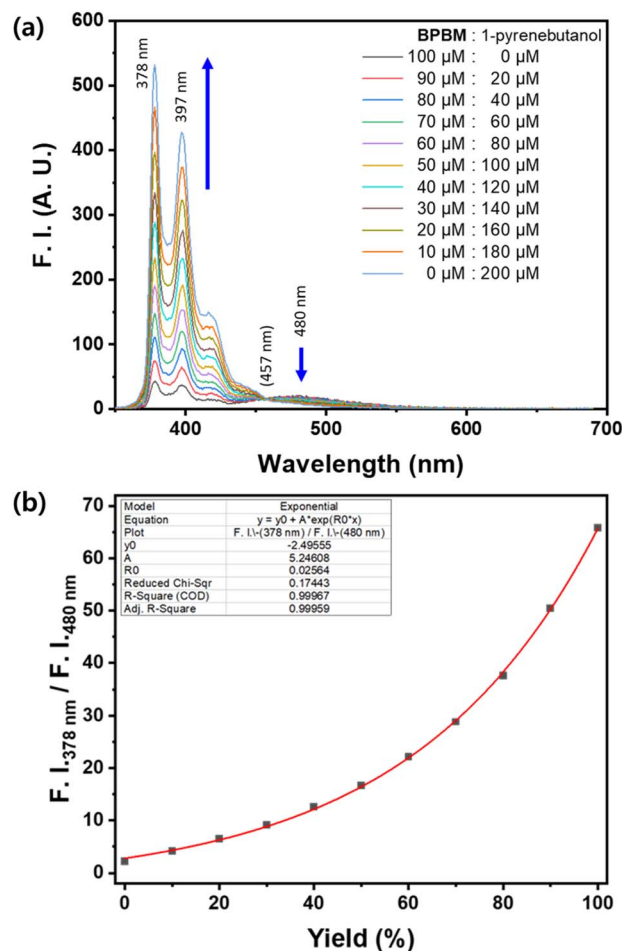


Fig. 2 (a) Fluorescence spectra of mixed solutions of **BPBM** probe and 1-pyrenebutanol product. The mixing ratio between the **BPBM** probe and 1-pyrenebutanol product depends on the progress of the transesterification reaction (excitation wavelength: 345 nm, excitation/emission slit width: 5 nm/5 nm, PMT: 500 V). (b) The plot of fluorescence intensity at 378 nm divided by fluorescence intensity at 480 nm versus various mixing ratios of the **BPBM** probe and 1-pyrenebutanol product depends on the progress of the transesterification reaction in chloroform and the calibration curve (red line). The yield of the reaction is calculated as  $\ln\{[(F. I. 378 \text{ nm} / F. I. 480 \text{ nm}) + 2.50] / 5.25\} / 0.0256$  (%).

research.<sup>58</sup> The catalytic activities of the prepared metal oxides were screened by transesterification reactions of 1  $\mu\text{mol}$  of **BPBM** with methanol in chloroform. The yields of the transesterification reactions were determined by measuring the fluorescent spectra of the reaction mixtures after 24 h reaction at 80  $^{\circ}\text{C}$ . Through three or more repeated experiments, copper, praseodymium, and samarium oxide catalysts showed high transesterification yields exceeding 60% under the screening conditions (Fig. 3). However, other transition or lanthanide metal oxides showed low yields of less than 50%. In particular, praseodymium oxide was selected as an outstanding hit catalyst, with a yield exceeding 80%. A powdered XRD pattern was obtained to characterize the selected praseodymium oxide (Fig. 4). The analysis revealed that the synthesized oxide had a cubic structure of praseodymium(IV) oxide ( $\text{PrO}_2$ ) rather than





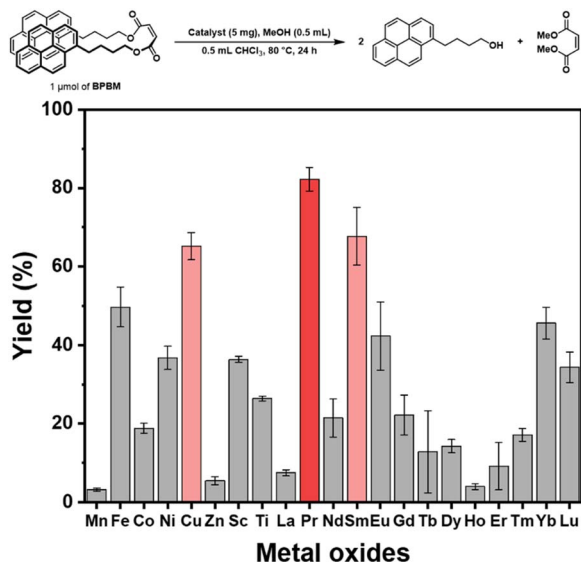


Fig. 3 Comparative fluorescence yields from transesterification using transition or lanthanide metal oxide catalysts with this HTS method.

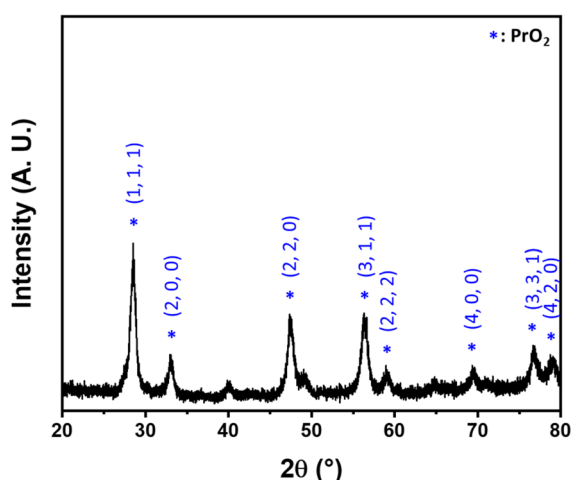


Fig. 4 XRD pattern of praseodymium oxide catalyst. The catalyst was found to have a cubic structure of PrO<sub>2</sub> by comparing the XRD pattern with the JCPDS 75-0152.

PrO, Pr<sub>2</sub>O<sub>3</sub>, or Pr<sub>6</sub>O<sub>11</sub>, and the XRD pattern correlated well with JCPDS 75-0152. The synthesized PrO<sub>2</sub> was analyzed using transmission electron microscopy (TEM), which demonstrated that the metal oxide was synthesized in the form of uniformly sized nanoparticles ranging from 10 to 20 nm (Fig. 5(a)–(c)) and confirmed its crystallinity (Fig. 5(d)). Elemental mapping images show that Pr and O are evenly distributed (Fig. S3†).

### Optimization of reaction conditions

Following the screening of the catalysts utilizing BPBM, the reaction conditions were optimized to conduct the transesterification reaction for various substrates using the selected PrO<sub>2</sub> catalyst. Benzyl benzoate (3aa) formation through the transesterification of methyl benzoate (1a) and benzyl alcohol

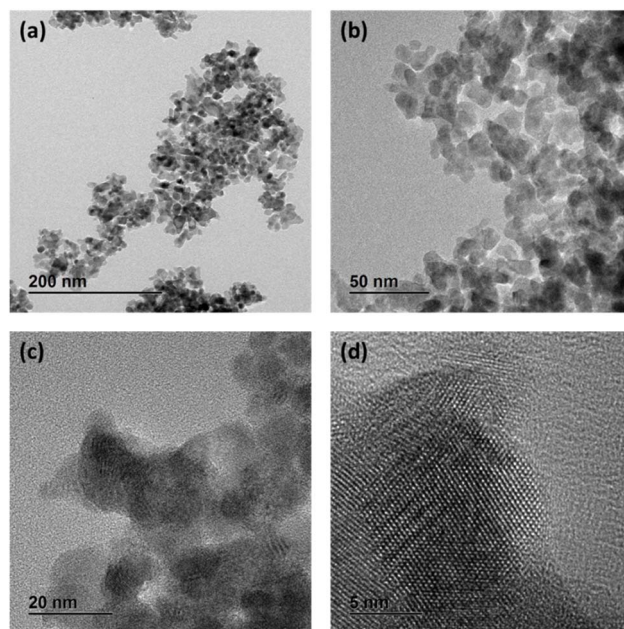


Fig. 5 TEM images of PrO<sub>2</sub> nanoparticle catalyst. (a)–(c) The particle size is uniformly distributed in the range of 10 to 20 nm. (d) The high-resolution TEM image confirms the crystallinity.

(2a) served as a model reaction. First, compared to the catalyst screening conditions (1  $\mu$ mol BPBM substrate, 5 mg catalyst), the amount of ester substrate (1a) was increased to 1.6 mmol, while the catalyst loading was slightly reduced. The reaction was conducted at 100 °C for 6 h using 2 mg of the PrO<sub>2</sub> catalyst without a solvent. However, almost no benzyl benzoate (3aa) was produced, and little conversion occurred (Table 1, entry 1). Despite the reaction time increasing to 12 h, only an insignificant amount of benzyl benzoate (3aa) was produced (entry 2). When the reaction temperature was raised to 150 °C, the yields were increased to 9% and 18% after 6 h and 12 h, respectively

Table 1 Reaction condition optimization for transesterification<sup>a</sup>

Entry	Catalyst loading (mg)	Temperature (°C)	Time (h)	Yield <sup>b</sup> (%)
1	2	100	6	0.3 <sup>c</sup>
2	2	100	12	0.9 <sup>c</sup>
3	2	150	6	9 <sup>c</sup>
4	2	150	12	18
5	2	200	6	95
6	– <sup>d</sup>	200	6	1.5 <sup>c</sup>
7	1	200	6	90
8	5	200	6	94

<sup>a</sup> Reaction conditions: 1.6 mmol of 1a and 3.2 mmol of 2a without solvent. <sup>b</sup> Isolated yield. <sup>c</sup> Calculated by NMR. <sup>d</sup> Without the catalyst.

Table 2 Comparison of different metal oxide catalysts for transesterification

Catalyst	Ester	Alcohol	Alcohol/ estemolar ratio	Catalyst loading <sup>a</sup>	Reaction temperature (°C)	Yield (%)	Reference
ZnO-Fe <sub>2</sub> O <sub>3</sub>	Methyl benzoate	Propanol	2	13.7 mg mmol <sup>-1</sup>	150	84	16
ZnO	Methyl nitrobenzoate	Ethanol	34	2 mol%	100	45	17
Cu/V <sub>2</sub> O <sub>5</sub>	Ethyl-10-undecenoate	Benzyl alcohol	2	5 mg mmol <sup>-1</sup>	100	78	18
TiO <sub>2</sub>	Dimethyl carbonate	Phenol	1	2.5 mg mmol <sup>-1</sup>	180	9	19
CeO <sub>2</sub>	Methyl benzoate	Octyl alcohol	1.2	20 mg mmol <sup>-1</sup>	160	97	25
Ti <sub>0.96</sub> Pr <sub>0.04</sub> O <sub>2</sub>	Propylene carbonate	Methanol	5	3.6 mg mmol <sup>-1</sup>	165	82	26
PrO <sub>2</sub>	Methyl benzoate	Benzyl alcohol	2	0.7 mol% or 1.25 mg mmol <sup>-1</sup>	200	95	This work

<sup>a</sup> Catalyst loading was expressed in mol% when specified; otherwise, it was given as the mass relative to the molar amount of the ester substrate.

(entries 3 & 4). Furthermore, an excellent yield of 95% was obtained in just 6 h or reaction at 200 °C (entry 5). In a control experiment without using catalyst, only a negligible conversion to **3aa** was observed (entry 6). This suggests that the reaction predominantly proceeds *via* catalysis, highlighting the necessity of the catalyst. When the catalyst loading was changed, the reaction yield using 1 mg of the PrO<sub>2</sub> catalyst decreased to 90%. However, the yield did not improve even when the amount of catalyst was increased to 5 mg (entries 7 & 8). Therefore, a suitable catalyst loading was determined to be 2 mg. To the best of our knowledge, the optimized catalyst loading (2 mg) represents the lowest amount used among the heterogeneous catalysts, corresponding to 0.7 mol% in molar ratio and 1.25 mg mmol<sup>-1</sup> by mass (Table 2).

### Substrate scope

Transesterifications were performed using various alcohols and esters under optimized conditions to evaluate the applicability of the catalyst to various substrates. Using primary benzyl alcohols (**2a**), the transesterification of methyl benzoate (**1a**) proceeded with an excellent yield of 95% within 6 h (Table 3, entry 1). This result demonstrates a higher yield in a shorter reaction time compared to reactions using other heterogeneous catalysts such as ZnCl<sub>2</sub>-hydroxyapatite,<sup>4</sup> CeO<sub>2</sub>,<sup>25</sup> maghemite-ZnO,<sup>16</sup> and oxidized carbon black,<sup>62</sup> with the same substrates (**1a** and **2a**). Despite the higher reaction temperature, the catalyst is advantageous because loading is the lowest among comparable reactions.<sup>4,16,25,62</sup> Halogen-substituted alcohol (**2b**) was well tolerated under the reaction conditions, with an excellent yield of 93% within 9 h (entry 2). However, regarding methoxybenzyl alcohol (**2c**), the reaction did not proceed because of side reactions, and the product was obtained in poor yield (entry 3). When methyl benzoate (**1a**) reacted with nitrobenzyl alcohol (**2d**), an excellent yield of 90% was obtained within 12 h (entry 4).

Aliphatic alcohols (**2e**, **2f**, **2g**) were also applied, and 1-hexanol (**2e**) and cyclohexanol (**2f**) reacted with methyl benzoate (**1a**) in excellent yields exceeding 90%, but long reaction times were required because the reactions were performed at 150 °C owing to the low boiling points of alcohols (entries 5 & 7). Nevertheless, this quantitative yield (**3af**) was significantly higher than the reaction using the same alcohol substrates (**2f**)

at the same temperature using Cu/V<sub>2</sub>O<sub>5</sub> catalyst.<sup>18</sup> In addition, for the reaction of 1-hexanol (**2e**), hexyl benzoate (**3ae**) was produced in a good yield of 72% at 150 °C within 48 h (entry 6). Meanwhile, cetyl alcohol (**2g**), which has a high boiling point, was tested under the optimized conditions, and an excellent yield of 91% was obtained within 16 h (entry 8). This result shows that the PrO<sub>2</sub> catalyst also catalyzes the transesterification of aliphatic alcohols well if the reaction temperature is sufficiently high.

The secondary benzyl alcohol, 1-phenylethanol (**2h**), reacted more slowly than the primary benzyl alcohols and a yield of 48% was observed in 38 h, and the low yield was also because the reaction could not proceed further owing to side reactions (entry 9). Nevertheless, this yield is significantly higher compared to a reported reaction using a Cu/V<sub>2</sub>O<sub>5</sub> catalyst with the same alcohol substrate (**2h**), which resulted in a negligible yield of 2%.<sup>18</sup> Transesterification were also attempted with tertiary alcohol (**2i**, **2j**), but *tert*-butanol (**2i**) did not react at 150 °C and 2-phenyl-2-propanol (**2j**) did not react at 200 °C either, likely due to steric hindrance. (entries 10 & 11). Referring to the results with the secondary benzyl alcohol, 1-phenylethanol (**2h**), where the reaction proceeded more slowly, it seems that higher steric hindrance tends to reduce reactivity.

Several methyl esters (**1b** and **1c**) were transesterified to benzyl esters (**3ba** and **3ca**) in yields exceeding 90% after 20 h (entries 12 & 13). Notably, a significantly higher yield was observed for methyl 4-nitrobenzoate (**1c**) compared to the moderate yield obtained in reactions with the ZnO catalyst using the same ester substrate.<sup>17</sup> However, methyl 4-aminobenzoate (**1d**) showed a low yield owing to side reactions (entry 14).

### Application to biodiesel production

After examining the substrate scope of the transesterification reaction catalyzed by PrO<sub>2</sub>, we determined that the catalyst could be utilized for biodiesel production. Biodiesel production involves the addition of methanol to long-chain triglycerides to form fatty acid methyl esters (FAMES) through transesterification. The reaction was conducted through a solvothermal reaction because methanol has a low boiling point. First, glyceryl trioctanoate, a single compound similar to the main component of vegetable oils, was tested. Using 2 mg of PrO<sub>2</sub> catalyst, a solvothermal reaction at 200 °C for 8 h yielded



Table 3 The substrate scope of PrO<sub>2</sub> nanoparticle catalysed transesterification<sup>a</sup>

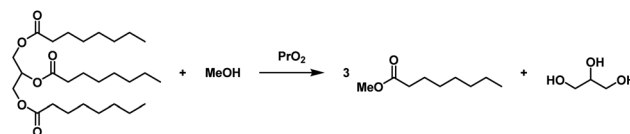
Entry	Ester (1)	Alcohol (2)	Product (3)	Temperature (°C)	Time (h)	Yield <sup>b</sup> (%)
1	1a	2a	3aa	200	6	95
2	1a	2b	3ab	200	9	93
3	1a	2c	3ac	200	6	40
4	1a	2d	3ad	200	12	90
5	1a	2e	3ae	150	219	91
6	1a	2e	3ae	150	48	72
7	1a	2f	3af	150	38	98
8	1a	2g	3ag	200	16	91
9	1a	2h	3ah	200	38	48
10	1a	2i	3ai	150	48	n. r. <sup>c</sup>
11	1a	2j	3aj	200	48	n. r. <sup>c</sup>
12	1b	2a	3ba	200	20	95
13	1c	2a	3ca	200	20	90
14	1d	2a	3da	200	20	21

<sup>a</sup> Reaction conditions: 1.6 mmol of ester (1), 3.2 mmol of alcohol (2), and 2 mg of PrO<sub>2</sub> nanoparticle catalyst without solvent. <sup>b</sup> Isolated yield. <sup>c</sup> No reaction.

74% methyl octanoate (Table 4, entry 1). When the catalyst was increased to 6 mg, the same product was obtained quantitatively (entry 2). Reducing the reaction time to 2 h and 4 h

resulted in yields of 58% and 74%, respectively (entries 3 & 4). On the other hand, soybean oil was reacted with methanol to investigate whether the selected catalyst could effectively



Table 4 Transesterification of triglycerides<sup>a</sup>

Entry	Substrate	Catalyst loading (mg)	Time (h)	Yield <sup>b</sup> (%)
1	Glyceryl trioctanoate	2	8	74
2	Glyceryl trioctanoate	6	8	99
3	Glyceryl trioctanoate	6	2	58
4	Glyceryl trioctanoate	6	4	74
5	Soybean oil	6	8	90 <sup>c</sup>
6	Soybean oil	- <sup>d</sup>	8	10 <sup>c</sup>

<sup>a</sup> Reaction conditions: 1.6 mmol of glyceryl trioctanoate or 0.8 mL of soybean oil and 16 mmol of methanol, solvothermal reaction at 200 °C without additional solvent. <sup>b</sup> Isolated yield. <sup>c</sup> Calculated by NMR. <sup>d</sup> Without the catalyst.

Table 5 Comparison of different metal oxide catalysts for biodiesel production

Catalyst	Feed stock	Methanol/oil molar ratio	Catalyst loading <sup>a</sup> (wt%)	Reaction temperature (°C)	Yield (%)	Reference
PbO, PbO <sub>2</sub>	Soybean oil	7	2	150	89	20
Ba-CaO	Waste cooking oil	6	1.0	65	98	21
CaO	Scum oil	13	0.9	60	96	22
Fe/Ba/Al <sub>2</sub> O <sub>3</sub>	Waste cooking oil	18	6	65	84	23
NiO/CaO	Waste cooking oil	18	6	65	97	24
La <sub>2</sub> O <sub>3</sub>	Rapeseed oil	28	10	200	98	27
La <sub>0.2</sub> Ce <sub>0.8</sub> O <sub>1.9</sub> -ZrO <sub>2</sub>	Waste cooking oil	15	5	120	91	28
Pr-CaO	Castor oil	8	2.5	65	87	29
PrO <sub>2</sub>	Soybean oil	12	0.8	200	90	This work

<sup>a</sup> Catalyst loading was expressed in wt% relative to the mass of the oil used.

produce biodiesel by transesterification of actual vegetable oils. The yield was calculated by comparing the ratio of the methyl peak of the methyl esters to the glyceryl peaks of the triglycerides in the <sup>1</sup>H NMR spectrum. As a result, 90% of the triglycerides were transformed to methyl esters after transesterification of soybean oil at 200 °C for 8 h using 6 mg of the PrO<sub>2</sub> catalyst (entry 5). In a control experiment without using catalyst, a simple thermal reaction yielded only 10% of methyl esters (entry 6). This indicates that the majority of the product is formed through the catalytic reaction, confirming that the catalyst is necessary for efficient biodiesel production. The mass of the catalyst used in the reaction was 0.8 wt% of the mass of soybean oil, demonstrating excellent yield with an insignificant amount of catalyst. To the best of our knowledge, this is the lowest catalyst loading reported for various metal oxide catalysts (Table 5).

## Conclusions

This study developed a fluorescence-based high-throughput screening method for transesterification reactions using a pyrene excimer probe. The method offers a fast and efficient way for catalyst developers to evaluate a wide range of

transesterification catalysts. The activities as transesterification catalysts of various transition or lanthanide metal oxide nanoparticles were quickly and efficiently analyzed. Praseodymium(IV) oxide, which shows the highest efficiency, was selected as the transesterification catalyst, and transesterification was performed on various substrates in high yields using this catalyst. In addition, the PrO<sub>2</sub> nanoparticles could catalyze the transesterification of triglycerides used in biodiesel production. Moreover, fatty acid methyl ester (FAME) was efficiently produced, even in soybean oil. The selected catalyst is advantageous owing to necessitating minimal amounts for the transesterification of various organic substrates (0.7 mol%) and soybean oil (0.8 wt%). The developed fluorescence-based assay method provides a valuable tool for rapid catalyst evaluation, offering a fast way to assess various transesterification catalyst candidates, including Lewis acids, bases, N-heterocyclic carbenes, and lanthanide doping or bimetallic oxides.

## Data availability

The data supporting this article have been included as part of the (ESI).†



## Author contributions

Conceptualization, M. S. H.; funding acquisition, M. S. H.; investigation, J. Y. R.; methodology, J. Y. R.; project administration, M. S. H.; resources, J. Y. R., M. J., T. L.; supervision, M. S. H.; writing—original draft, J. Y. R.; writing—review and editing, J. Y. R. and M. S. H. All authors have read and agreed to the published version of the manuscript.

## Conflicts of interest

There are no conflicts to declare.

## Acknowledgements

This work was supported by the National Research Foundation of Korea (NRF) grant funded by the Korea government (MSIT) (RS-2023-00220174).

## References

- 1 J. Otera, *Chem. Rev.*, 1993, **93**, 1449–1470.
- 2 J. Otera, *Acc. Chem. Res.*, 2004, **37**, 288–296.
- 3 J. W. J. Bosco and A. K. Saikia, *Chem. Commun.*, 2004, 1116–1117, DOI: [10.1039/B401218F](https://doi.org/10.1039/B401218F).
- 4 A. Solhy, J. H. Clark, R. Tahir, S. Sebti and M. Larzek, *Green Chem.*, 2006, **8**, 871–874.
- 5 T. Ohshima, T. Iwasaki, Y. Maegawa, A. Yoshiyama and K. Mashima, *J. Am. Chem. Soc.*, 2008, **130**, 2944–2945.
- 6 S.-S. Weng, C.-S. Ke, F.-K. Chen, Y.-F. Lyu and G.-Y. Lin, *Tetrahedron*, 2011, **67**, 1640–1648.
- 7 D. A. Watson, X. Fan and S. L. Buchwald, *J. Org. Chem.*, 2008, **73**, 7096–7101.
- 8 S. R. Jagtap, M. D. Bhor and B. M. Bhanage, *Catal. Commun.*, 2008, **9**, 1928–1931.
- 9 J. Chen, E. Namila, C. Bai, M. Baiyin, B. Agula and Y.-S. Bao, *RSC Adv.*, 2018, **8**, 25168–25176.
- 10 J. J. Newton, R. Britton and C. M. Friesen, *J. Org. Chem.*, 2018, **83**, 12784–12792.
- 11 G. A. Grasa, R. M. Kissling and S. P. Nolan, *Org. Lett.*, 2002, **4**, 3583–3586.
- 12 G. W. Nyce, J. A. Lamboy, E. F. Connor, R. M. Waymouth and J. L. Hedrick, *Org. Lett.*, 2002, **4**, 3587–3590.
- 13 G. A. Grasa, T. Güveli, R. Singh and S. P. Nolan, *J. Org. Chem.*, 2003, **68**, 2812–2819.
- 14 R. Singh, R. M. Kissling, M.-A. Letellier and S. P. Nolan, *J. Org. Chem.*, 2004, **69**, 209–212.
- 15 T. Zeng, G. Song and C.-J. Li, *Chem. Commun.*, 2009, 6249–6251, DOI: [10.1039/B910162D](https://doi.org/10.1039/B910162D).
- 16 V. B. Gade, A. K. Rath, S. B. Bhalekar, J. Tucek, O. Tomanec, R. S. Varma, R. Zboril, S. N. Shelke and M. B. Gawande, *ACS Sustain. Chem. Eng.*, 2017, **5**, 3314–3320.
- 17 M. M. A. Soliman, E. C. B. A. Alegria, A. P. C. Ribeiro, M. M. Alves, M. S. Saraiva, M. Fátima Montemor and A. J. L. Pombeiro, *Dalton Trans.*, 2020, **49**, 6488–6494.
- 18 S. Sudhakaran, A. Taketoshi, S. M. A. H. Siddiki, T. Murayama and K. Nomura, *ACS Omega*, 2022, **7**, 4372–4380.
- 19 L. Tan, Y. Huang, W. Mao, X. Hu, Y. Huang, H. Chen and X. Luo, *Ind. Eng. Chem. Res.*, 2024, **63**, 16347–16355.
- 20 A. K. Singh and S. D. Fernando, *Energy Fuels*, 2008, **22**, 2067–2069.
- 21 J. Boro, L. J. Konwar, A. J. Thakur and D. Deka, *Fuel*, 2014, **129**, 182–187.
- 22 K. N. Krishnamurthy, S. N. Sridhara and C. S. Ananda Kumar, *Renewable Energy*, 2020, **146**, 280–296.
- 23 N. F. Sulaiman, A. N. N. Hashim, S. Toemen, S. J. M. Rosid, W. N. A. W. Mokhtar, R. Nadarajan and W. A. W. A. Bakar, *Renewable Energy*, 2020, **153**, 1–11.
- 24 N. F. Sulaiman, N. I. Ramly, M. H. Abd Mubin and S. L. Lee, *RSC Adv.*, 2021, **11**, 21781–21795.
- 25 M. Tamura, S. M. A. Hakim Siddiki and K.-I. Shimizu, *Green Chem.*, 2013, **15**, 1641–1646.
- 26 S. Dahiya, V. C. Srivastava and V. Kumar, *Energy Fuels*, 2022, **36**, 13148–13158.
- 27 B. M. E. Russbuehl and W. F. Hoelderich, *J. Catal.*, 2010, **271**, 290–304.
- 28 M. Afsharizadeh and M. Mohsennia, *Fuel*, 2021, **304**, 121350.
- 29 S. Gohar Khan, M. Hassan, M. Anwar, Z. Sheikh, U. Masood Khan and C. Zhao, *Fuel*, 2022, **330**, 125480.
- 30 Y. Uozumi and Y. Nakai, *Org. Lett.*, 2002, **4**, 2997–3000.
- 31 X.-B. Jiang, P. W. N. M. van Leeuwen and J. N. H. Reek, *Chem. Commun.*, 2007, 2287–2289, DOI: [10.1039/B700156H](https://doi.org/10.1039/B700156H).
- 32 O. Trapp, *J. Chromatogr.*, 2008, **1184**, 160–190.
- 33 C. Cai, J. Y. L. Chung, J. C. McWilliams, Y. Sun, C. S. Shultz and M. Palucki, *Org. Process Res. Dev.*, 2007, **11**, 328–335.
- 34 H. Fang, Q. Xiao, F. Wu, P. E. Floreancig and S. G. Weber, *J. Org. Chem.*, 2010, **75**, 5619–5626.
- 35 M. T. Reetz, M. H. Becker, H.-W. Klein and D. Stöckigt, *Angew. Chem., Int. Ed.*, 1999, **38**, 1758–1761.
- 36 J. W. Szewczyk, R. L. Zuckerman, R. G. Bergman and J. A. Ellman, *Angew. Chem., Int. Ed.*, 2001, **40**, 216–219.
- 37 C. Markert and A. Pfaltz, *Angew. Chem., Int. Ed.*, 2004, **43**, 2498–2500.
- 38 M. T. Reetz, A. Eipper, P. Tielmann and R. Mynott, *Adv. Synth. Catal.*, 2002, **344**, 1008–1016.
- 39 K. Mori, Y. Ichikawa, M. Kobayashi, Y. Shibata, M. Yamanaka and T. Akiyama, *Chem. Sci.*, 2013, **4**, 4235–4239.
- 40 O. Lavastre and J. P. Morken, *Angew. Chem., Int. Ed.*, 1999, **38**, 3163–3165.
- 41 M. Kawatsura and J. F. Hartwig, *Organometallics*, 2001, **20**, 1960–1964.
- 42 O. Löber, M. Kawatsura and J. F. Hartwig, *J. Am. Chem. Soc.*, 2001, **123**, 4366–4367.
- 43 D. F. Kennedy, B. A. Messerle and S. L. Rumble, *New J. Chem.*, 2009, **33**, 818–824.
- 44 E. Jung, S. Kim, Y. Kim, S. H. Seo, S. S. Lee, M. S. Han and S. Lee, *Angew. Chem., Int. Ed.*, 2011, **50**, 4386–4389.
- 45 S. Kim, E. Jung, M. J. Kim, A. Pyo, T. Palani, M. S. Eom, M. S. Han and S. Lee, *Chem. Commun.*, 2012, **48**, 8751–8753.





- 46 A. Pyo, S. Kim, M. R. Kumar, A. Byeun, M. S. Eom, M. S. Han and S. Lee, *Tetrahedron Lett.*, 2013, **54**, 5207–5210.
- 47 M. S. Eom, J. Noh, H.-S. Kim, S. Yoo, M. S. Han and S. Lee, *Org. Lett.*, 2016, **18**, 1720–1723.
- 48 H.-S. Kim, M. S. Eom, M. S. Han and S. Lee, *Chem.–Eur. J.*, 2017, **23**, 6282–6285.
- 49 Y. Son, S. Lee, H.-S. Kim, M. S. Eom, M. S. Han and S. Lee, *Adv. Synth. Catal.*, 2018, **360**, 3916–3923.
- 50 K. H. Shaughnessy, P. Kim and J. F. Hartwig, *J. Am. Chem. Soc.*, 1999, **121**, 2123–2132.
- 51 J. P. Stambuli, S. R. Stauffer, K. H. Shaughnessy and J. F. Hartwig, *J. Am. Chem. Soc.*, 2001, **123**, 2677–2678.
- 52 S. R. Stauffer, N. A. Beare, J. P. Stambuli and J. F. Hartwig, *J. Am. Chem. Soc.*, 2001, **123**, 4641–4642.
- 53 S. R. Stauffer and J. F. Hartwig, *J. Am. Chem. Soc.*, 2003, **125**, 6977–6985.
- 54 G. Angelovski, M. D. Keränen, P. Linnepe, S. Grudzielanek and P. Eilbracht, *Adv. Synth. Catal.*, 2006, **348**, 1193–1199.
- 55 H.-M. Guo and F. Tanaka, *J. Org. Chem.*, 2009, **74**, 2417–2424.
- 56 B. Xia, B. Gerard, D. M. Solano, J. Wan, G. Jones II and J. A. Porco Jr., *Org. Lett.*, 2011, **13**, 1346–1349.
- 57 H. Noh, T. Lim, B. Y. Park and M. S. Han, *Org. Lett.*, 2020, **22**, 1703–1708.
- 58 T. Lim and M. S. Han, *Catalysts*, 2020, **10**, 542.
- 59 T. Lim, J. Y. Ryoo, M. Jang and M. S. Han, *Org. Biomol. Chem.*, 2021, **19**, 1009–1016.
- 60 J. Y. Ryoo and M. S. Han, *Org. Biomol. Chem.*, 2024, **22**, 6103–6107.
- 61 J. Zheng, W. Wei, X. Lan, Y. Zhang and Z. Wang, *Anal. Biochem.*, 2018, **549**, 26–28.
- 62 M. R. Acocella, M. Maggio, C. Ambrosio, N. Aprea and G. Guerra, *ACS Omega*, 2017, **2**, 7862–7867.

